ISSN 1674-1056
http://cpb.iphy.ac.cn
http://iopscience.iop.org/cpb
中国物理 B
Chinese Physics
中国物理 Chinese Physics B

Temperature-dependent subband mobility characteristics in n-doped silicon junctionless nanowire transistor

Ya-Mei Dou(窦亚梅), Wei-Hua Han(韩伟华), Yang-Yan Guo(郭仰岩), Xiao-Song Zhao(赵晓松), Xiao-Di Zhang(张晓迪), Xin-Yu Wu(吴歆宇), Fu-Hua Yang(杨富华)

Citation: Chin. Phys. B . 2019, 28(6): 066804. **doi:** 10.1088/1674-1056/28/6/066804
Journal homepage: http://cpb.iphy.ac.cn; http://iopscience.iop.org/cpb

What follows is a list of articles you may be interested in

Surface effects on the thermal conductivity of silicon nanowires

Hai-Peng Li(李海鹏), Rui-Qin Zhang(张瑞勤)

Chin. Phys. B . 2018, 27(3): 036801. **doi:** 10.1088/1674-1056/27/3/036801

A review for compact model of graphene field-effect transistors

Nianduan Lu(卢年端), Lingfei Wang(汪令飞), Ling Li(李泠), Ming Liu(刘明)

Chin. Phys. B . 2017, 26(3): 036804. **doi:** 10.1088/1674-1056/26/3/036804

Growth condition optimization and mobility enhancement through inserting AlAs monolayer in the InP-based $In_xGa_{1-x}As/In_{0.52}Al_{0.48}As$ HEMT structures

Shu-Xing Zhou(周书星), Ming Qi(齐鸣), Li-Kun Ai(艾立鹍), An-Huai Xu(徐安怀)

Chin. Phys. B . 2016, 25(9): 096801. **doi:** 10.1088/1674-1056/25/9/096801

Performance improvement in polymeric thin film transistors using chemically modified both silver bottom contacts and dielectric surfaces

Xie Ying-Tao, Ouyang Shi-Hong, Wang Dong-Ping, Zhu Da-Long, Xu Xin, Tan Te, Fong Hon-Hang

Chin. Phys. B . 2015, 24(9): 096803. **doi:** 10.1088/1674-1056/24/9/096803

Growth condition optimization and mobility enhancement throughprolonging the GaN nuclei coalescence process of AlGaN/AlN/GaN structure

He Xiao-Guang, Zhao De-Gang, Jiang De-Sheng, Zhu Jian-Jun, Chen Ping, Liu Zong-Shun, Le Ling-Cong, Yang Jing, Li Xiao-Jing, Zhang Shu-Ming, Yang Hui

Chin. Phys. B . 2015, 24(9): 096802. **doi:** 10.1088/1674-1056/24/9/096802

Temperature-dependent subband mobility characteristics in n-doped silicon junctionless nanowire transistor*

Ya-Mei Dou(窦亚梅)[1,2], Wei-Hua Han(韩伟华)[1,2,†], Yang-Yan Guo(郭仰岩)[1,2], Xiao-Song Zhao(赵晓松)[1,2], Xiao-Di Zhang(张晓迪)[1,2], Xin-Yu Wu(吴歆宇)[1,2], and Fu-Hua Yang(杨富华)[1,2,3]

[1] *Engineering Research Center for Semiconductor Integration Technology & Beijing Engineering Center of Semiconductor Micro-Nano Integrated Technology, Institute of Semiconductors, Chinese Academy of Sciences, Beijing* 100083, *China*

[2] *Center of Materials Science and Optoelectronics Engineering, University of Chinese Academy of Sciences, Beijing* 100049, *China*

[3] *State Key Laboratory for Superlattices and Microstructures, Institute of Semiconductors, Chinese Academy of Sciences, Beijing* 100083, *China*

(Received 6 March 2019; revised manuscript received 29 March 2019; published online 8 May 2019)

We have investigated the temperature-dependent effective mobility characteristics in impurity band and conduction subbands of n-doped silicon junctionless nanowire transistors. It is found that the electron effective mobility of the first subband in 2-fold valleys is higher than that of the second subband in 4-fold valleys. There exists a maximum value for the effective subband mobilities at low temperatures, which is attributed to the increase of thermally activated electrons from the ionized donors in the impurity band. The experimental results indicate that the effective subband mobility is temperature-dependent on the electron interactions by thermal activation, impurity scattering, and intersubband scattering.

Keywords: effective subband mobility, thermal activation, Coulomb scattering, silicon nanowire transistor

PACS: 68.65.La, 68.65.Hb, 05.60.Gg, 11.40.–q **DOI:** 10.1088/1674-1056/28/6/066804

1. Introduction

The metal–oxide–semiconductor field-effect transistor (MOSFET) has kept pace with Moore's law by improving the "performance/power" ratio since 2000. New materials, such as strained silicon,[1] high-k dielectric and metal gate electrodes,[2] are introduced in the complementary metal–oxide–semiconductor (CMOS) process to increase the carrier mobility. However, as the space of pn junctions in source and drain drops to less than 10 nm, there is a great challenge in the fabrication of pn junctions with heavily doping concentration gradients. In recent years, the silicon junctionless nanowire transistor (JNT) with uniform doping in source, drain, and channel has attracted much attention due to the simple fabrication and unique properties, in which the narrow conduction channel emerges in the axis of the silicon nanowire. Compared with the inversion-mode transistors, JNTs have less degradation of mobility and more apparent quantum-confinement effects on carrier transport.[3,4] Therefore, it is necessary to understand the strong oscillatory behaviors of carrier effective mobility in the quantized subband structure. Yamada *et al.* estimated the subband mobility of quasi-two-dimensional electrons in Si atomic layer doped GaAs for the first time, in which the subband mobility difference was up to 20:1.[5] Each new subband filling results in an increased intersubband Coulomb scattering, thus a reduced mobility. Colinge *et al.* measured the subband mobility of trigate silicon-on-insulator (SOI) MOSFETs to reach about 1200 $cm^2/(V{\cdot}s)$ due to screening of impurity scattering at the temperature of 4.4 K, which decreases as temperature increases.[6] The Coulomb scattering is temperature-dependent for thermally activated carriers between impurity band and conductive subbands. Yi *et al.* observed quantum confinement effects of sub-5-nm thick p-Si junctionless nanowire (NW) field-effect transistors (FETs) at room temperature.[4] The hole mobility is increased in p-SiNW FETs, which is caused by minimal acoustic phonon assisted intersubband scattering. In this paper, we investigate temperature-dependent effective mobility characteristics in impurity band and conduction subbands of n-doped silicon JNT. Interestingly, the electron effective mobility of conduction subbands has a maximum value at low temperatures, which relates to the minimum electron effective mobility of the impurity band. The effective subband mobility is temperature-dependent on the electron interactions by thermal activation, impurity scattering, and intersubband scattering.

2. Device fabrication and characterization

The device in Fig. 1(a) was fabricated on the (100)-orientated SOI wafer, with the top silicon thickness of 55 nm and buried oxide layer of 145 nm. First, the top silicon layer was implanted under SiO_2 buffer layer with 33-keV arsenic ions at a dose of 2×10^{12} cm^{-2}. Following the implantations, the silicon nanowire along the $\langle 110 \rangle$ direction was defined by electron beam lithography (EBL) and reactive ion etching (RIE). The width of the nanowire was about 60 nm, which was measured by scanning electron microscope (SEM).

*Project supported by the National Key Research and Development Program of China (Grant No. 2016YFA0200503).

†Corresponding author. E-mail: weihua@semi.ac.cn

© 2019 Chinese Physical Society and IOP Publishing Ltd

Then the silicon nanowire was oxidized at 900 °C for 10 min in dry oxygen ambience to form an SiO_2 layer. Next, SiO_2 layer was removed by buffered oxide etcher (BOE) for 40 s to reduce the size of silicon nanowire and remove the etching damage. Subsequently, the 22-nm-thick gate dielectric layer was generated on the surface of silicon nanowires by thermal oxidation. The 200-nm-thick undoped polysilicon layer was then deposited by low-pressure chemical vapor deposition (LPCVD). The polysilicon layer was oxidized at 900 °C for 30 min in oxygen ambience to form a 15 nm-thick SiO_2 layer. The poly-Si layer was implanted with 33-keV boron ions at the dose of 2×10^{12} cm^{-2}, followed by furnace annealing at 1000 °C for 15 s. Following the implantations, the polycrystalline gate pattern was defined by EBL and inductively couple plasma (ICP) etching. Then, a 200 nm-thick SiO_2 passivation layer was deposited by LPCVD. Finally, the source, drain, and gate electrodes were fabricated. Figure 1(b) shows the top view SEM image of the device. We measured the JNT electrical characterization with an Agilent B1500 A semiconductor parameter analyzer within the temperature range from 6 K to 250 K.

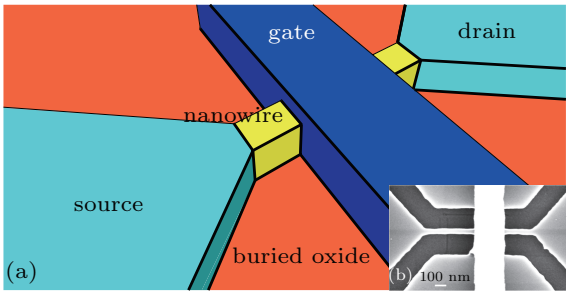


Fig. 1. (a) The schematic structure and (b) top-view SEM image of the silicon junctionless nanowire transistor.

3. Results and discussion

Figure 2 shows the measured drain current I_{ds} in the JNT device as a function of gate voltage V_g and temperatures at the bias $V_{ds} = 10$ mV in both linear and log scales. Clear oscillatory peaks and several step-like drain current features are observed at the initial stage of the I_{ds}–V_g transfer characteristics, implying the evolution of electron transport behaviors from quantum dots to quantum wire. The initial drain current below the gate voltage of about 2.3 V flows through an ultranarrow channel in the center axis of silicon nanowire, in which several ionized dopant atoms work as quantum dots in an array. With the gate voltage increasing, the dopant barrier potentials are reduced in the wider channel, thereby enhancing the coupling of dopant-induced quantum dots. The Fermi energy level is allowed to enter the conduction subbands in the quantum confined one-dimensional channel. The step-like current features at the gate voltages of around 2.5 V and 2.8 V result from the successive filling of individual subband. Each current step corresponds to the filling of a new subband. However, as the temperature increases up to 100 K, the current oscillation features gradually decrease and disappear due to the weak potential confinement in conduction channel.

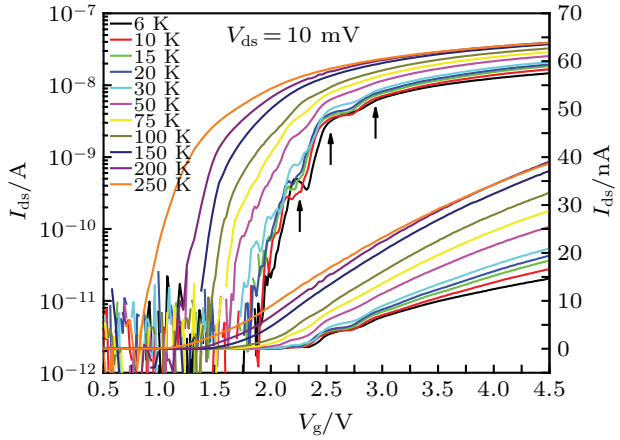


Fig. 2. Drain current I_{ds} *versus* gate voltage V_g with bias $V_{ds} = 10$ mV at different temperatures.

Figure 3(a) shows that several remarkable oscillation peaks at initial conductance varies with the gate voltage within the temperature range from 6 K to 50 K, which are successively shifted in the conductance for clarity. Only one oscillation peak is observed at the temperature of 6 K, which results from electron tunneling through the level in only one donor-induced quantum dot. Under the gate electric field, the electrons self-consistently fill in the D^- level state of the neutral donor atom, which is much closer to the top of the barrier along the transport direction due to screened donor potential.[7] As the temperature rises, thermally activated electrons are able to hop through the optimal neighbor dopant atoms. Several split peaks are observed in the temperature range from 10 K to 50 K in Fig. 3(a), resulting from the coupling effect in the dopant-induced quantum dot array. To show this more clearly, the drain current I_{ds} and transconductance g_m curves are presented in Fig. 3(b) as a function of gate voltage V_g in different bias V_{ds} from 3 mV to 10 mV at the temperature of 30 K. Two groups of double oscillation current peaks can be observed at the gate voltage of 1.95 V and 2.13 V, resulting from the electrons tunneling through the D^0 and D^- states of the two ionized donors. As a result, according to the spacing of the gate voltage $\Delta V_{gs} = 0.18$ V between the D^0 and D^- states of current peaks, we estimate the gate capacitance $C_g = e/\Delta V_{gs} = 0.89$ aF for single dopant-induced quantum dot with the potential radius of 1.54 nm.

Figure 4 provides three remarkable temperature-dependent peaks of the transconductance g_m ($= \partial I_{ds}/\partial V_g|_{V_{ds}=\text{const}}$), which are extracted from the temperature-dependent transfer characteristic curves in Fig. 2. It can be observed that the g_m-peak positions in the gate voltage V_g are basically stable with the temperature increasing, corresponding to the step positions of the drain-current I_{ds}. At the

temperature of 6 K, the first transconductance peak at the gate voltage of about 2.13 V originates from the electron tunneling through the D^- level of dopant-induced quantum dots. The second and third transconductance peaks at the gate voltages of about 2.44 V and 2.86 V correspond to the electron one-dimensional transport in the first and second conduction subbands, which are the lowest subbands respectively in the 2-fold perpendicular valleys and the 4-fold in-plane valleys of the strain silicon nanowire.[8]

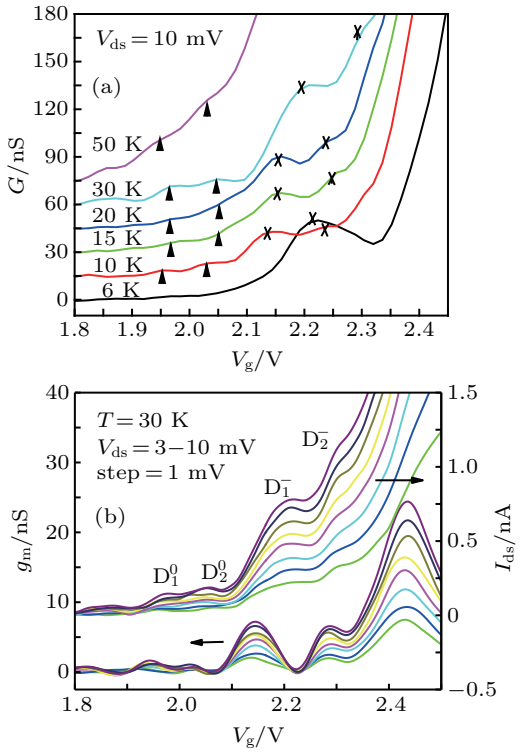


Fig. 3. (a) The conductance G varies with the gate voltage V_g in $V_{ds} = 10$ mV at different temperatures. The curves are successively shifted in the conductance for clarity. (b) The transconductance g_m versus the gate voltage V_g and the transfer characteristic curve I_{ds}–V_g in $V_{ds} = 3$ mV–10 mV at the temperature of 30 K.

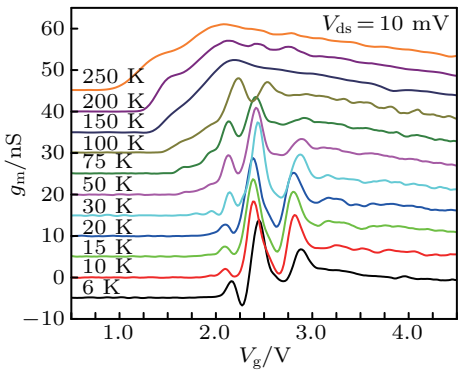


Fig. 4. Temperature-dependent transconductance g_m–V_g curves, which are successively shifted for clarity.

In order to understand the interaction mechanism between the impurity band and the conduction subbands, we further investigate the dependence of effective electron mobility on the temperatures. Similar to the definition of the effective electron mobility in inversion-mode MOSFETs in the triode operation regime, the effective mobility in linear accumulation regime of the silicon JNT can be estimated by[4,9–11]

$$\mu_{\text{eff}} = \frac{g_m L_g}{C_{ox} W_{\text{eff}} V_{ds}},$$

where $L_g = 280$ nm is the gate length, $C_{ox} = 1.56 \times 10^{-7}$ F/cm^2 is the gate capacitance per unit area, and the effective width W_{eff} is defined as twice the height H, plus the width W of nanowire. Figure 5 shows the evolution of the effective mobilities as a function of temperature for the impurity band and conduction subbands (in the inset). It can be observed that the effective electron mobility μ_{e0} at the D^- level in the impurity band is the lowest at the temperature of 10 K, in which the thermally activated electrons are delocalized from the ionized donor atoms. The effective electron mobility μ_{e0} of the impurity band is reduced below 10 K by the impurity Coulomb scattering, and then enhanced above 10 K by the increased thermal activation energy of electrons. Therefore, the lowest effective mobility μ_{e0} at 10 K results from the interaction of thermal activation and impurity scattering.[10] As a result, the concentration of activated electrons hopping into the conduction subbands rapidly increases with the temperature increasing.

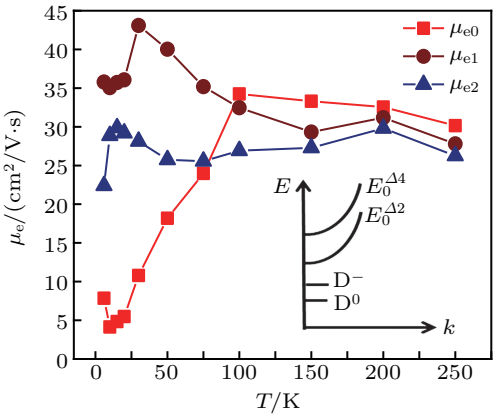


Fig. 5. The temperature-dependent effective mobilities of the impurity band and the conduction subbands. The inset is the diagram of the energy band.

The effective subband mobilities μ_{e1} and μ_{e2} have the largest value at the temperature of 30 K and 15 K, respectively, due to the increased electron concentration and intersubband Coulomb scattering. The effective subband mobility enhancement is attributed to the increase of activated electrons in the occupancy of conduction subbands.[12] The effective mobility μ_{e1} in the first subband is higher than the μ_{e2} in the second subband, because the effective electron mass in 2-fold valleys is lower than that in 4-fold valleys. The successive filling of individual subband strengthens the intersubband scattering with Fermi energy moving up, further reducing the effective subband mobilities. It is also interesting that the effective mobility of impurity band is higher than that of subbands as the temperature is higher than 100 K, which is attributed to the phonon scattering. This means that the intersubband Coulomb scattering of conduction subbands is stronger than that of the

impurity band when the phonon interaction is dominant. The phonon-limited mobilities show the slowly declined tendency with temperature increasing above 100 K.

4. Conclusions

In conclusion, we have demonstrated the temperature dependence of effective mobility in impurity band and conduction subbands of the n-type junctionless silicon nanowire transistor. The minimum effective mobility of impurity band at the temperature of 10 K results from the interaction of thermal activation for electrons and impurity scattering. The electron effective mobility of the first subband in 2-fold valleys is higher than that of the second subband in 4-fold valleys. The maximum effective subband mobility at the low temperature is attributed to increased electron concentration and intersubband Coulomb scattering. It is found that the phonon scattering plays a dominant role in both impurity band and conduction subbands above the temperature of 100 K, leading to a slow decline in electron effective mobility.

Acknowledgment

The authors thank Mr. Li Xiao-Ming, Dr. Zhang Yan-Bo, Ma Liu-Hong, and Wang Hao for their technical support in device fabrication.

References

[1] Niquet Y M, Delerue C and Krzeminski C 2012 *Nano Lett.* **12** 3545
[2] Cassé M, Tachi K, Thiele S and Ernst T 2010 *Appl. Phys. Lett.* **96** 123506
[3] Colinge J P, Lee C W, Afzalian A, Akhavan N D, Yan R, Ferain I, Razavi P, O'Neill B, Blake A, White M, Kelleher A M, McCarthy B and Murphy R 2010 *Nat. Nanotechnol.* **5** 225
[4] Yi K S, Trivedi K, Floresca H C, Yuk H, Hu W and Kim M J 2011 *Nano Lett.* **11** 5465
[5] Yamada S and Makimoto T 1990 *Appl. Phys. Lett.* **57** 1022
[6] Colinge J P, Quinn A J, Floyd L, Redmond G, Alderman J C, Xiong W Z, Cleavelin C R, Schulz T, Schruefer K, Knoblinger G and Patruno P 2006 *IEEE Electron Dev. Lett.* **27** 120
[7] Fuechsle M, Miwa J A, Mahapatra S, Ryu H, Lee S, Warschkow O, Hollenberg L C L, Klimeck G and Simmons M Y 2012 *Nat. Nanotechnol.* **7** 242
[8] Ma L H, Han W H, Wang H, Yang X and Yang F H 2015 *IEEE Electron Dev. Lett.* **36** 941
[9] Ford A C, Ho J C, Chueh Y L, Tseng Y C, Fan Z, Guo J, Bokor J and Javey A 2009 *Nano Lett.* **9** 360
[10] Li X, Han W, Wang H, Ma L, Zhang Y, Du Y and Yang F 2013 *Appl. Phys. Lett.* **102** 223507
[11] Cui Y, Duan X F, Hu J T and Lieber C M 2000 *J. Phys. Chem. B* **104** 5213
[12] Rustagi S C, Singh N, Lim Y F, Zhang G, Wang S, Lo G Q, Balasubramanian N and Kwong D L 2007 *IEEE Electron Dev. Lett.* **28** 909